Structure-Based Optimization of Pyrazolo[3,4-*d*]pyrimidines as Abl Inhibitors and Antiproliferative Agents toward Human Leukemia Cell Lines

Fabrizio Manetti,[†] Chiara Brullo,[‡] Matteo Magnani,[†] Francesca Mosci,[§] Beatrice Chelli,[||] Emmanuele Crespan,[⊥] Silvia Schenone,*[,‡] Antonella Naldini,[§] Olga Bruno,[‡] Maria Letizia Trincavelli,[||] Giovanni Maga,[⊥] Fabio Carraro,[§] Claudia Martini,[||] Francesco Bondavalli,[‡] and Maurizio Botta[†]

Dipartimento Farmaco Chimico Tecnologico, Università degli Studi di Siena, Via Alcide de Gasperi 2, I-53100, Siena, Italy, Dipartimento di Scienze Farmaceutiche, Università degli Studi di Genova, Viale Benedetto XV 3, I-16132, Genova, Italy, Dipartimento di Fisiologia, Sezione di Neuroimmunofisiologia, Università degli Studi di Siena, Via Aldo Moro, I-53100, Siena, Italy, Dipartimento di Psichiatria, Neurobiologia, Farmacologia e Biotecnologie, Università di Pisa, Via Bonanno 6, I-56126, Italy, and Istituto di Genetica Molecolare, IGM-CNR, Via Abbiategrasso 207, I-27100, Pavia, Italy

Received October 1, 2007

Results from molecular docking calculations and Grid mapping laid the foundations for a structure-based optimization approach to improve the biological properties of pyrazolo-pyrimidine derivatives in terms of inhibition of Abl enzymatic activity and antiproliferative properties toward human leukemia cells. Insertion of halogen substituents with various substitution patterns, suggested by simulations, led to a significant improvement of leukemia cell growth inhibition and to an increase up to 1 order of magnitude of the affinity toward Abl.

Introduction

Chronic myelogenous leukemia (CML[a]) is a disease characterized by the presence of the Philadelphia chromosome (discovered in 1960 by Nowell and Hungerford)[1] and results from a reciprocal translocation between chromosomes 9 and 22.[2] This translocation fuses the breakpoint cluster region (Bcr) and the Abelson kinase (Abl) genes, forming the *Bcr-Abl* oncogene[3] that encodes the constitutively active cytoplasmatic tyrosine kinase (TK) Bcr-Abl, present in >90% of CML.[4] Bcr-Abl causes hyperproliferation of the stem cells and the consequent pathology of the disease that progresses through three phases (chronic proliferative phase, accelerated phase, and blast crisis phase), becoming more resistant to treatment in each successive phase. The last phase is also characterized by the presence of genomic instability and is ultimately fatal.[5]

The finding that Bcr-Abl is the cause of the leukemic phenotype and that the tyrosine kinase activity of Abl is fundamental for Bcr-Abl-mediated transformation made this kinase an important target for the development of specific therapies. In 1996, Novartis reported the first potent ATP-competitive Abl kinase inhibitor, **1** (Chart 1).[6] It was approved by the Food and Drug Administration (FDA) in 2001 and became, within a few years of its discovery, the first line therapy, generally well tolerated for the treatment of CML. In the chronic phase, **1** is highly effective toward CML, with excellent and durable hematological and cytological responses in the majority of patients. Nevertheless, primary refractoriness and acquired resistance to this drug are observed frequently in patients in the accelerated phase or blast crisis. The two main mechanisms of resistance are the overexpression of Bcr-Abl, mainly due to gene amplification,[7] and, more frequently, mutations in the kinase domain of Bcr-Abl.[8]

Second generation Abl inhibitors were synthesized through rational drug design approaches to overcome resistance to **1**.[9] Recently, Novartis disclosed **2** (Chart 1), structurally related to **1**, which showed promising results in preclinical studies and was 10–25-fold more potent compared to **1** in cellular assays. Compound **2** also inhibited the growth of cell lines expressing Bcr-Abl mutants resistant to **1**.[10] On the other hand, unlike **1** and its derivatives, **3** (Chart 1) is a substrate binding site Abl inhibitor that inhibits wild type kinase 10-fold more potently than **1**, and it also has activity against kinase domain mutations resistant to **1**.[11]

A different potential therapeutic approach for CML is based on the study of Bcr-Abl/Src dual inhibitors,[12–14] taking into consideration that the activity of Src is elevated in the presence of the Bcr-Abl oncoprotein. Compound **4** (Chart 1) is an ATP-competitive thiazole-carboxamide derivative, 100–300-fold more active than **1** and orally active in CML animal models.[15,16a] This compound was recently approved by the FDA with the name of Sprycel for the treatment of all phases of CML in adults with resistance or intolerance to prior therapy, including **1**.[17] Moreover, very recently **4** was tested in vitro and in vivo against the pediatric preclinical testing program with promising results.[16b] Another promising molecule (**5**, Chart 1) is a purine compound synthesized with the help of mutagenesis studies and molecular modeling simulations, which inhibits both native and **1**-resistant mutations. Unfortunately, this compound shows nonspecific cytotoxicity.[18] Moreover, **6** (Chart 1) is a potent and selective dual Bcr-Abl/Lyn (a Src TK family member) inhibitor. Although structurally similar to **1**, **6** is 25–55-fold more potent, and it is also active on the Bcr-Abl mutated form, but not on the T315I mutation.[19,20] Finally, **7** (Chart 1) was

* To whom correspondence should be addressed. Telephone: 0039 010 3538866. Fax: 0039 010 3538358. E-mail: schensil@unige.it.

[†] Dipartimento Farmaco Chimico Tecnologico, Università degli Studi di Siena.

[‡] Dipartimento di Scienze Farmaceutiche, Università degli Studi di Genova.

[§] Dipartimento di Fisiologia, Sezione di Neuroimmunofisiologia, Università degli Studi di Siena.

[||] Dipartimento di Psichiatria, Neurobiologia, Farmacologia e Biotecnologie, Università di Pisa.

[⊥] Istituto di Genetica Molecolare, IGM-CNR.

[a] Abbreviations: CML, chronic myelogenous leukemia; Bcr, breakpoint cluster region; TK, tyrosine kinase; Abl, Abelson kinase; FDA, Food and Drug Administration; MIFs, molecular interaction fields; STAT-5, signal transducer and activator of transcription 5; HRI, hydrophobic region I; HRII, hydrophobic region II.

10.1021/jm701240c CCC: $40.75
Published on Web 02/08/2008

Chart 1. Schematic Representation of Current Available Inhibitors of Abl (**1**−**7**) and PP2 (**8**, Used as Reference Compound in Enzymatic and Cellular Assays Reported in the Paper)

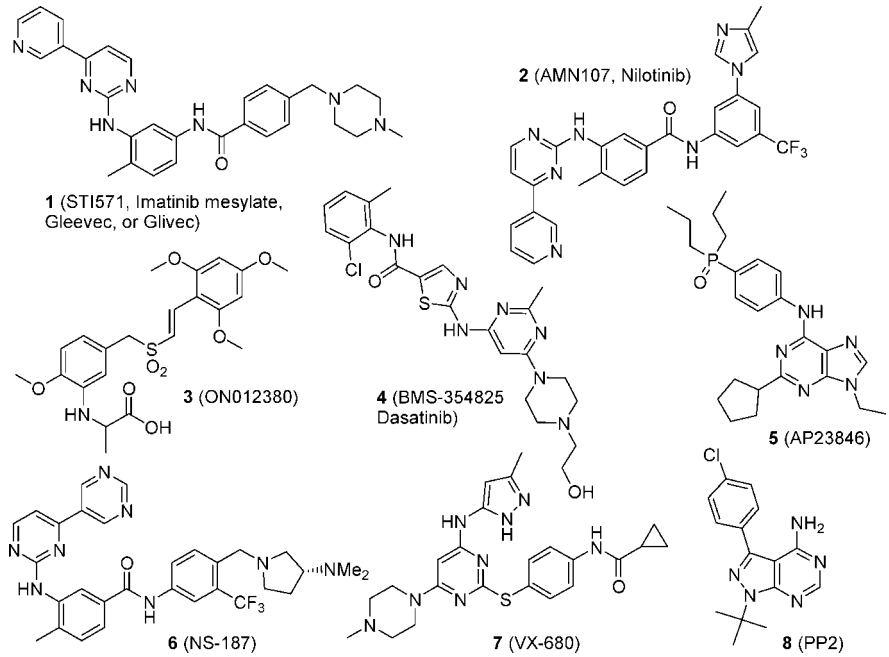

reported very recently as a small molecule inhibitor of the Aurora kinase, which also inhibits Abl at low nanomolar concentrations.[21]

In this context, we have recently published a series of pyrazolo[3,4-*d*]pyrimidine derivatives endowed with inhibitory activity toward the c-Abl enzyme.[22] Continuing our efforts in this research field, we describe in this paper the rational design and the synthesis of second generation derivatives showing a significant improvement of their activity profile against both isolated Abl and leukemia cells, in comparison to the parent compounds.

Docking simulations on the original series of pyrazolo-pyrimidines[22] indicated two different binding modes of the inhibitors within the ATP binding pocket of Abl, depending on the presence or not of an alkylthio substituent at the C6 position of the heterocyclic nucleus. However, in both cases, the occupancy of the two main hydrophobic regions (hereafter referred to as hydrophobic regions I and II and reported as HRI and HRII) of the ATP binding pocket seemed to play a crucial role in determining affinity toward Abl. In addition to this finding, a detailed analysis of the binding site was performed with the aim of identifying additional regions of favorable interactions between inhibitors and the protein not exploited by the first series of ligands. For this purpose, molecular interaction fields (MIFs) were calculated for the binding site by means of the software Grid.[23] Briefly, Grid inserts the macromolecular target under investigation (the binding site region of Abl) into a grid and then computes, at each node of the grid, the interaction energies between several probes (atoms or groups of atoms representing various chemical functionalities found in the inhibitor structures) and the target itself. The set of energy values calculated for a specific probe constitutes the MIFs of the probe−target system.

Details derived from both docking studies and Grid analysis were then combined together, thus suggesting structural modifications that should allow the location of a certain inhibitor substituent in a region of favorable interaction with the protein. Based on this structural information, we chose to introduce substituents on both of the phenyl rings at positions N1 and C4 (in an attempt to fulfil the additional space available within both HRI and HRII), while keeping the pyrazolo-pyrimidine core intact. As an example, Figure 1A shows the binding mode of a compound of the original series, namely **21** ($K_i = 0.4\ \mu$M toward isolated Abl, Table 1), as determined by docking experiments. Regions of minimum interaction energy (i.e., the most favorable interaction points) for probe Cl (organic chlorine atom, magenta) and F (organic fluorine atom, cyan) are also displayed. The binding mode is characterized by the location of the side chains at N1 and C4 within the HRI and HRII, respectively. Moreover, N5 and the NH moiety of the inhibitor are engaged in hydrogen bond contacts with the backbone NH and the carbonyl group of Met318, respectively. Additional information is provided by MIFs which show the presence of minima for Cl and F probes located within both of the hydrophobic pockets surrounding the phenyl moieties of inhibitors. This finding suggests the synthesis of a set of derivatives bearing halogen substituents with different substitution patterns on one or both of the aromatic rings of the inhibitors. Accordingly, compounds **9**−**20** were synthesized as reported in Scheme 1.

Chemistry. The starting compounds **22a**−**c**, prepared from the appropriate hydrazine and ethyl(ethoxymethylene)cyanacetate, were reacted with formamide for 8 h at 190 °C to give the corresponding pyrazolo[3,4-*d*]pyrimidinones **23a**−**c** in high yields. Treatment of the latter with an excess of the Vilsmeier complex ($POCl_3$/DMF, 1:1) for 12 h at reflux in $CHCl_3$ led to the formation of the halogenated derivatives **24a**−**c**. The C4 chlorine atom was in turn substituted with the appropriate benzylamine, in anhydrous toluene at room temperature (rt), to afford the final compounds **9**−**20** in yields ranging between 65% and 80% (Table 1).

Results and Discussion

The new compounds were then submitted to biological tests to evaluate their affinity toward the Abl enzyme in a cell-free assay and their antiproliferative activity in cellular assays on three human leukemia cell lines (namely, K-562, MEG-01, and KU-812), in comparison to **8** (PP2, Chart 1), chosen

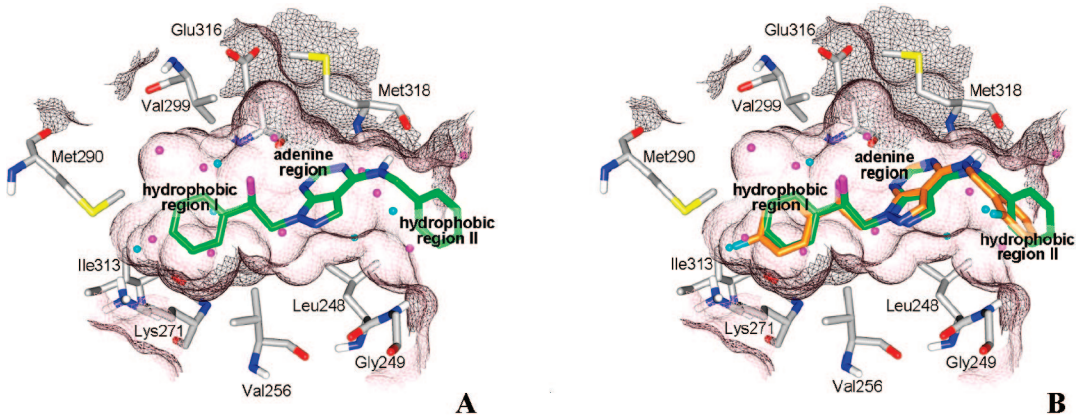

Figure 1. Graphical representation of the binding mode of pyrazolo[3,4-*d*]pyrimidines within the ATP binding pocket of c-Abl (mesh representation of the surface). Regions of minimum energy as derived from molecular interaction field calculations are also displayed for probes Cl (magenta spheres) and F (cyan spheres). (A) Binding mode of **21** (green, $K_i = 0.4$ μM toward isolated Abl) and **15** (orange, $K_i = 0.02$ μM toward isolated Abl). The fluorine substituents of **15** are both at close contact with regions of minimum energy (cyan spheres) for the F probe, suggesting profitable interactions between ligand and target.

Table 1. Structure and Inhibitory Activity of Compounds **9–21** toward Isolated Abl Kinase and Human Leukemia K-562, MEG-01, and KU-812 Cell Lines

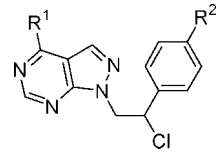

					IC$_{50}$ (μM)		
compd	R^1	R^2	Caco-2[a]	K_i (μM)[b]	K-562[c]	MEG-01[d]	KU-812[c]
8 (PP2)				0.50 ± 0.20	25 ± 3	17 ± 1	45 ± 3
9	NHCH$_2$(*p*-F-Ph)	H	0.72	2.0 ± 0.1	114 ± 13	8.4 ± 0.4	
10	NHCH$_2$(*m*-F-Ph)	H	0.72	0.04 ± 0.01	46 ± 6	14 ± 2	
11	NHCH$_2$(*o*-F-Ph)	H	0.71	0.73 ± 0.05	79 ± 5	8.5 ± 1.5	
12	NHBn	F	0.80	0.44 ± 0.06	26 ± 4	11 ± 5	16 ± 2
13	NHCH$_2$(*p*-F-Ph)	F	0.53	0.20 ± 0.03	58 ± 7	12 ± 3	
14	NHCH$_2$(*m*-F-Ph)	F	0.55	0.10 ± 0.02	35 ± 3	12 ± 3	
15	NHCH$_2$(*o*-F-Ph)	F	0.55	0.02 ± 0.01	36 ± 2	15 ± 1	
16	NHCH$_2$(*m*-Cl-Ph)	F	0.84	0.12 ± 0.01	12 ± 2	14 ± 2	38 ± 2
17	NHCH$_2$(*o*-Cl-Ph)	F	0.91	0.20 ± 0.04	34 ± 5	18 ± 1	
18	NHCH$_2$(*p*-F-Ph)	Cl	0.69	0.08 ± 0.04	9 ± 1	5.5 ± 1.4	8 ± 1
19	NHCH$_2$(*p*-Cl-Ph)	Cl	1.16		37 ± 5	9.7 ± 1.5	
20	NHCH$_2$(*m*-Cl-Ph)	Cl	0.94	0.08 ± 0.01	36 ± 2	5.0 ± 1.5	
21[e]	NHBn	H	1.06	0.40 ± 0.06	48 ± 4	63 ± 5	

[a] Caco-2 refers to the Caco2 permeation model (as implemented in Volsurf).[24] Values represent a score ranging from −1 to +1, corresponding to the following permeability values: −1 corresponds to a permeability $<4 \times 10^{-6}$ cm/s; 0 corresponds to a permeability between 4×10^{-6} and 8×10^{-6} cm/s; 1 corresponds to a permeability $>8 \times 10^{-6}$ cm/s. [b] K_i values toward isolated Abl calculated according to the following equation: $K_i = ID_{50}/\{E_0 + [E_0(K_{m(ATP)}/S_0)]\}/E_0$, where E_0 and S_0 are the enzyme and the ATP concentrations (0.005 and 0.012 μM, respectively). [c] IC$_{50}$ values are means ± SD of five experiments, each performed in triplicate. [d] IC$_{50}$ values are means ± standard error of three experiments, each performed in duplicate. [e] Reported elsewhere.[26]

Scheme 1[a]

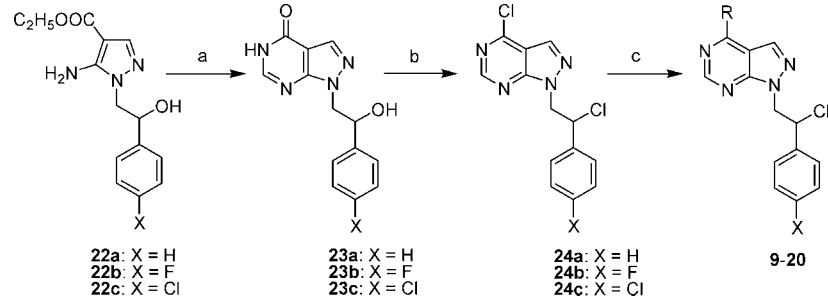

[a] Reagents: (a) Formamide, 190 °C, 8 h; (b) POCl$_3$/DMF, CHCl$_3$, reflux, 12 h; (c) benzylamines, anhydrous toluene, rt, 48 h.

as the reference compound. As a result, cellular activity underwent a significant improvement (Table 1), and the enzymatic affinity ameliorated up to 1 order of magnitude, in comparison with biological data of the corresponding nonhalogenated parent compounds. As expected by previous docking studies, halogenated derivatives adopted the binding mode found for 6-unsubstituted pyrazolo-pyrimidines, while halogen substituents were in most cases located in regions

of space where Grid analysis found profitable interactions between halogen atoms and the target. As an example, a comparison between the binding mode of **15** (the most active compound toward Abl, among the pyrazolo-pyrimidines synthesized by us) and **21** (Figure 1B) showed the same orientation within the ATP binding pocket of Abl, with fluorine substituents of **15** that lie in regions of space corresponding to points of minimum energy found by Grid for the F probe. Such additional contacts allowed us to account for the higher affinity of **15** (0.02 μM) with respect to its congeneric analogues **14** and **13** (showing K_i values of 0.10 and 0.20 μM, respectively) with a different substitution pattern on the phenyl ring at C4. In fact, their *m*-F and *p*-F substituents at R^1 (Table 1) were accommodated into portions of HRII where no minima for the F probe were found. Similarly, **17** and **16** showed a reduced affinity for Abl because their *o*- and *m*-Cl substituents at R^1, respectively, are unable to profitably interact with minima for the Cl probe within HRII. Moreover, also **12**, due to the lack of any substituent on the phenyl ring of the C4 benzylamino moiety, was unable to make additional profitable contacts with HRII and, consequently, showed a reduced affinity (0.44 μM).

By changing the F substituent (at R^2) of **16** into a Cl to give **20**, affinity toward Abl underwent only a slight variation from 0.12 to 0.08 μM, respectively. An analysis of the location of MIF maps showed that this result was probably due to the fact that the interaction pathway of **16** and **20** was very similar. In fact, no changes occurred within HRII, where the *m*-Cl-benzylamino group of both compounds is located. On the other molecular edge, the F substituent at R^2 of **16**, interacting with a F minimum within HRI, was replaced by a Cl group of **20** that, in turn, was able to contact a Cl minimum in the same region of HRI, leading to an unchanged interaction pathway. Similarly, when transforming **13** (0.20 μM) into **18** (0.08 μM), a 2.5-fold difference in affinity was found. Compounds **9** (2.0 μM) and **11** (0.73 μM), lacking the F substitution at the phenyl ring on N1, showed a marked reduction in affinity toward Abl, at least 1 order of magnitude lower with respect to the corresponding fluoro derivatives **13** (0.2 μM) and **15** (0.02 μM), respectively. The affinity of **10** (0.04 μM), which was better than that of the corresponding F analogue **14** (0.10 μM), was an exception to this trend, and it was impossible to be rationalized on the sole basis of computational results.

The new compounds were found to have an antiproliferative activity toward three human leukemia cell lines in the range from low micromolar to micromolar concentration (Table 1), and all of the cell lines seemed to be equally sensitive to the treatment with the inhibitors. However, **18** showed the best biological profile in terms of antiproliferative properties and affinity toward Abl, although **15** had a 4-fold better affinity (0.02 μM of **15** versus 0.08 μM of **18**).

It is important to point out that an analysis of biological data revealed some discrepancies between enzymatic and cellular activity. As an example, compound **15**, showing the best inhibitory activity in the enzymatic assay (0.02 μM), was about 3–4-fold less potent than **18** (showing a comparable activity in the enzymatic assay, 0.08 μM) in cell-based assays. In an attempt to rationalize these data, compounds were projected on an in silico permeability model (a mathematical model describing the ability of compounds to permeate Caco2 cells) implemented within the Volsurf software.[24] Results showed that, in principle, compounds were well absorbed through cell membranes, with several differences. In fact, **15** exhibited a lower permeability in comparison to **18**, accounting for its lower cellular activity. Similarly, **12** and **16** showed permeability values among the highest of the whole set, which could account for the fact that they were two of the most active compounds in cellular assays, despite their relatively low enzymatic potency (0.44 and 0.12 μM, respectively).

On the basis of experimental results, **18** was selected as a hit to perform additional biological assays aimed at better understanding the antiproliferative activity of this compound toward leukemia cells. In particular, to check if the antiproliferative effect of **18** toward each cell line was dependent on the inhibition of Bcr-Abl activity, we evaluated the phosphorylation of both Bcr-Abl and its downstream substrate STAT-5 (Bcr-Abl is known to phosphorylate STAT-5, a transcription factor directly activating Bcl-xL, which works as an apoptosis inhibitor at the mitochondrial level) in addition to the phosphorylation of Src. As a result, on K-562 cells, **18** markedly reduced Src phosphorylation with respect to control and showed an activity also better than that of PP2 (Figure 2A and D, left). Moreover, Bcr-Abl phosphorylation was potently inhibited (significantly better than PP2) by **18** (Figure 2A and B, left), which was also able to reduce STAT-5 phosphorylation at a higher extension with respect to PP2 (Figure 2A and C, left). In a similar way, Bcr-Abl phosphorylation of KU-812 cells was strongly and equally inhibited by both **18** and PP2 (Figure 2A and B, right). Moreover, **18** was also able to greatly reduce phosphorylation of both STAT-5 (Figure 2A and C, right) and Src (Figure 2A and D, right) better than the reference compound PP2. In summary, immunoblot analysis of lysates from compound-treated cells with specific antiphospho antibodies revealed a reduction in phosphorylation of all of the targets. Taken together, reduction of the phosphorylation levels of both Bcr-Abl and STAT-5 strongly suggested that effects mediated by **18** on proliferation and apoptosis of leukemia cells are a consequence of the reduction of Bcr-Abl kinase activity.

Moreover, inhibition of STAT-5 phosphorylation by means of **18** and involvement of STAT-5 in apoptosis control via Bcl-xL led to the suggestion to investigate the expression of Bax/Bcl-xL mRNA in the leukemia cells under study. For this purpose, it is well-known that the ratio between Bax mRNA and Bcl-xL mRNA expression may be used as a direct index of the induction of the apoptotic process (the proapoptotic action of Bax is antagonized by Bcl-xL) and could help in explaining the molecular mechanism of apoptosis induction. Accordingly, upon incubation of K-562 and KU-812 cells for 72 h in the presence of **18** (Figure 3B and C), a marked increase in the Bax/Bcl-xL ratio was evidenced, confirming induction of leukemia cells toward apoptosis. Moreover, exposure of K-562 cells to **18** for 3 h also strongly affected the ratio between Bax mRNA and Bcl-xL mRNA expression (Figure 3A).

In conclusion, the previous knowledge of the binding mode of pyrazolo[3,4-*d*]pyrimidines into the ATP binding site of Abl (predicted on the basis of docking studies) was combined with a detailed analysis of the binding pocket (performed with the software Grid) to provide suggestions for the synthesis of novel derivatives with improved affinity toward the macromolecular target. Results of cellular and enzymatic assays performed on the new compounds demonstrated that structural modifications led to an overall improvement of the inhibitory activities with respect to the corresponding dehalogenated parent compounds. In particular, **18** emerged as a hit with an antiproliferative activity toward Bcr-Abl-positive human leukemia cells significantly ameliorated and with an

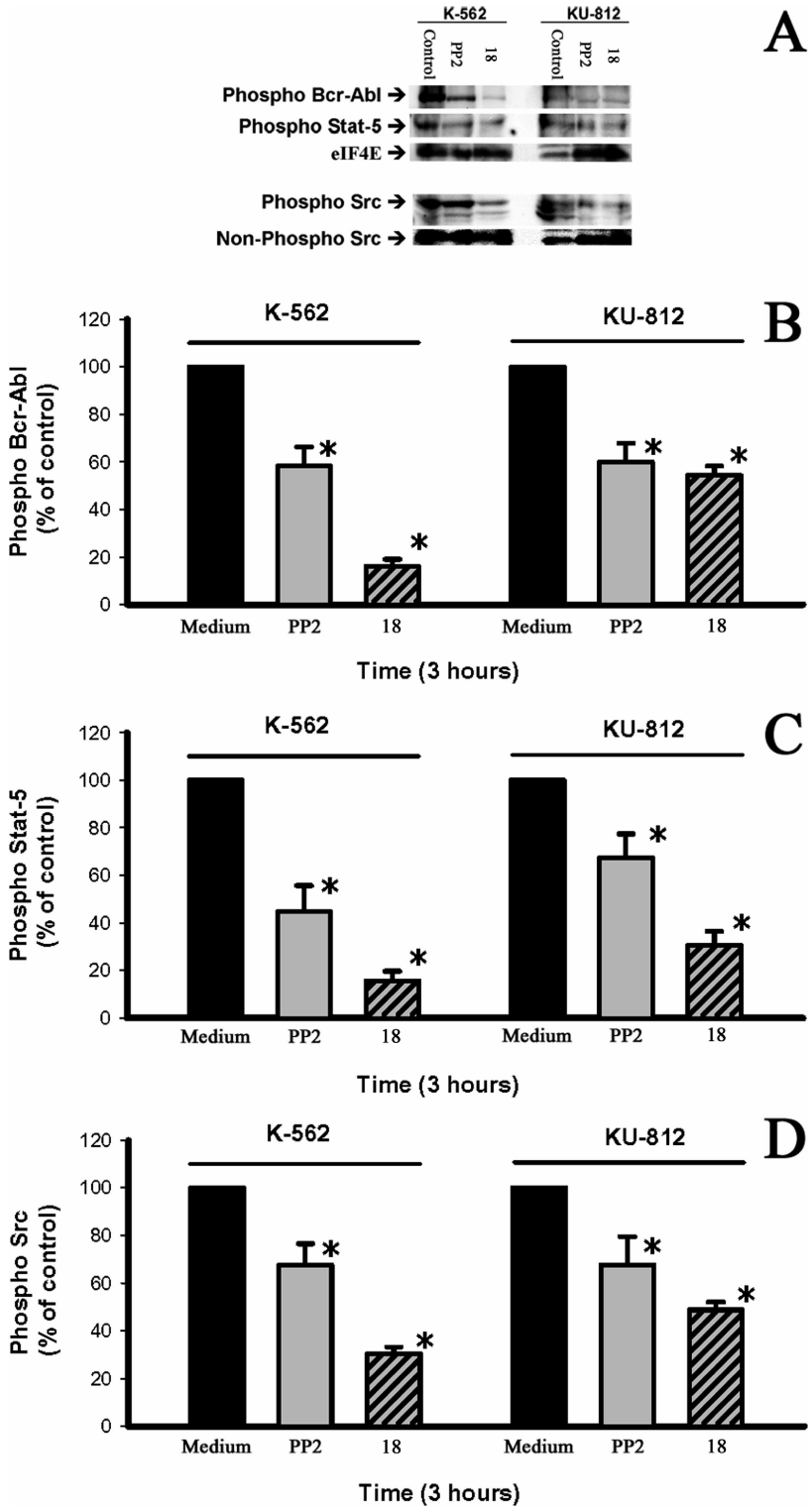

Figure 2. Compound **18** reduces phosphorylation of Bcr-Abl, STAT-5, and Src. (A) Effects of **18** on the phosphorylation of phospho Bcr-Abl, phospho STAT-5, and phospho Src in K-562 and KU-812 cells, in comparison to PP2 used as the reference compound. The quantification is shown in panels B, C, and D. Results are expressed as the mean ± SEM of three independent experiments. Asterisks indicate statistically significant ($p < 0.05$) differences between the inhibition of phophorylation due to treatment with **18** and PP2 versus untreated cell lines, as determined by using the Student's *t* test and the Bonferroni's correction.

affinity toward isolated Abl up to more than 1 order of magnitude higher with respect to previous compounds. At the molecular level, it was able to inhibit phosphorylation of both Bcr-Abl and its downstream target STAT-5, thus interfering in the apoptotic process regulated by the balance between Bax and Bcl-xL. On the basis of these experimental findings, identification of **18** allows a step forward in the design of new antileukemia agents.

Experimental Details

A. Chemistry. Starting materials were purchased from Aldrich-Italia (Milan, Italy).

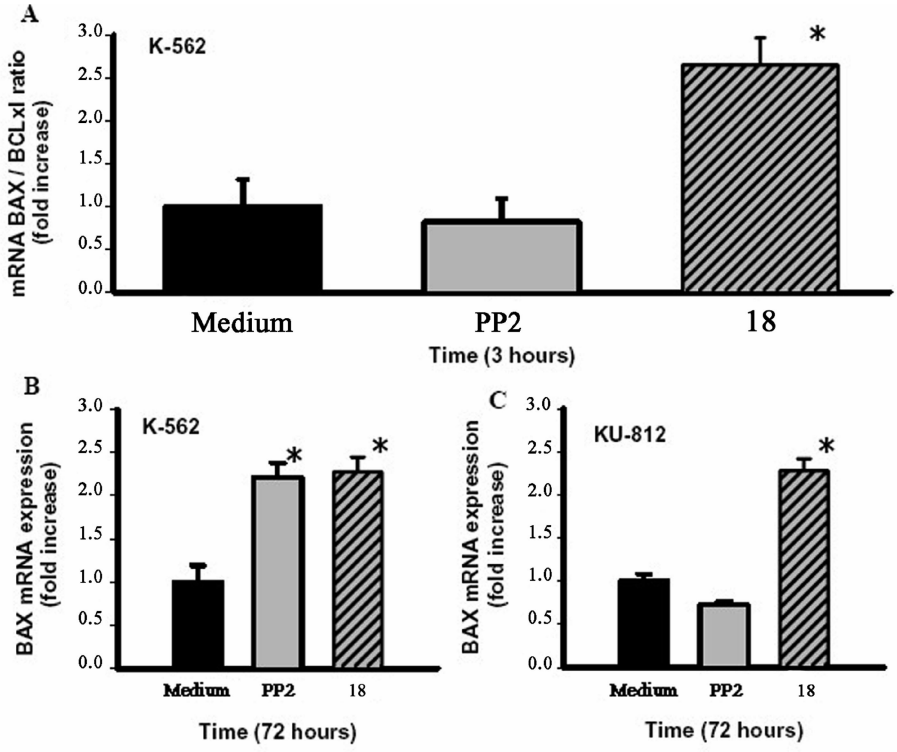

Figure 3. Compound **18** induces a proapoptic response on CML cell lines. (A) Exposure to **18** for 3 h affects the ratio of Bax/Bcl-xL mRNA expression in K-562. The expression of Bax mRNA is also significantly enhanched after a 72 h exposure to the compound in (B) K-562 and (C) KU-812 cells, respectively. The means ± SEM of four independent experiments are presented. Bax and Bcl-xL mRNA expression in compound-treated cells was determined by qRT-PCR. All values were expressed as fold increase relative to the expression of β-Actin. Asterisks indicate statistically significant ($p < 0.05$) differences between the medium and the investigated compound.

Melting points were determined with a Büchi 530 apparatus and are uncorrected. IR spectra were measured in KBr with a Perkin-Elmer 398 spectrophotometer. ^{1}H NMR spectra were recorded in a $(CD_3)_2SO$ solution on a Varian Gemini 200 (200 MHz) instrument. Chemical shifts are reported as δ (ppm) relative to TMS as internal standard, with J in Hz. ^{1}H patterns are described using the following abbreviations: s = singlet, d = doublet, t = triplet, q = quartet, m = multiplet, and br = broad. All compounds were tested for purity by TLC (Merck, Silica gel 60 F_{254}, $CHCl_3$ as the eluant). Analyses for C, H, and N were within ±0.3% of the theoretical values.

Synthesis and analytical data of intermediates **22a**, **23a**, and **24a** were already reported.[25]

1. General Procedure for the Synthesis of Ethyl 5-Amino-1-[2-(4-halophenyl)-2-hydroxyethyl]-1*H*-pyrazole-4-carboxylates (22b,c). The appropriate hydrazine (20 mmol) was added to a solution of ethyl(ethoxymethylene)cyanacetate (3.38 g, 20 mmol) in anhydrous toluene (20 mL) and the mixture was heated at 80 °C for 8 h. The solution was concentrated under reduced pressure to half of the volume and allowed to cool to rt. The yellow pale solid was filtered and recrystallized from toluene to afford **22b**,**c** as white solids.

2. Ethyl 5-Amino-1-[2-(4-fluorophenyl)-2-hydroxyethyl]-1*H*-pyrazole-4-carboxylate (22b). Yield 70%, mp 163–164 °C. ^{1}H NMR: δ 1.33 (t, J = 7.0, 3H, CH_3), 3.73 (br s, 1H, OH, disappears with D_2O), 3.90–4.15 (m, 2H, CH_2N), 4.29 (q, J = 7.0, 2H, CH_2O), 5.01–5.18 (m, 1H, CHO), 5.36 (br s, 2H, NH_2, disappears with D_2O), 7.03–7.40 (m, 4H Ar), 7.55 (s, 1H, H-3). IR (cm^{-1}): 3448, 3446 (NH_2), 3300–3000 (OH), 1685 (CO). Anal. ($C_{14}H_{16}N_3O_3F$) C, H, N.

3. General Procedure for the Synthesis of 1-[2-(4-Halophenyl)-2-hydroxyethyl]-1,5-dihydro-4*H*-pyrazolo[3,4-*d*]pyrimidin-4-ones (23b,c). A suspension of **22b** or **22c** (10 mmol) in formamide (10 g, 333 mmol) was heated at 190 °C for 8 h and then poured in H_2O (300 mL). The crude product was filtered and purified by dissolving in 2 M NaOH (100 mL) and boiling with charcoal, followed by precipitation with glacial acetic acid. The solid was filtered and recrystallized from absolute ethanol to give compounds **23b** or **23c** as white solids.

4. 1-[2-(4-Fluorophenyl)-2-hydroxyethyl]-1,5-dihydro-4*H*-pyrazolo[3,4-*d*]pyrimidin-4-one (23b). Yield 73%, mp 281–282 °C (dec). ^{1}H NMR: δ 4.22–4.35 and 4.39–4.54 (2m, 2H, CH_2N), 5.02–5.17 (m, 1H, CHO), 5.72 (br s, 1H, OH, disappears with D_2O), 7.03–7.19 and 7.24–7.38 (2m, 4H Ar), 8.02 (s, 1H, H-3), 8.07 (s, 1H, H-6), 12.13 (br s, 1H, NH, disappears with D_2O). IR (cm^{-1}): 3387 (NH), 3168–2900 (OH), 1737 (CO). Anal. ($C_{13}H_{11}N_4O_2F$) C, H, N.

5. General Procedure for the Synthesis of 4-Chloro-1-[2-chloro-2-(4-halophenyl)ethyl]-1*H*-pyrazolo[3,4-*d*]pyrimidines (24b,c). The Vilsmeier complex, previously prepared from $POCl_3$ (15.33 g, 100 mmol) and anhydrous dimethylformamide (DMF) (7.31 g, 100 mmol) was added to a suspension of compound **23b** or **23c** (10 mmol) in $CHCl_3$ (50 mL). The mixture was refluxed for 12 h. After cooling at rt, the mixture was washed with H_2O (2 × 20 mL), dried ($MgSO_4$), filtered, and concentrated under reduced pressure. The crude oil was purified by column chromatography (Florisil, 100–200 mesh) using diethyl ether as the eluant, to afford the pure products **24b** or **24c** as white solids.

6. 4-Chloro-1-[2-chloro-2-(4-fluorophenyl)ethyl]-1*H*-pyrazolo[3,4-*d*]pyrimidine (24b). Yield 75%, mp 128–129 °C. ^{1}H NMR: δ 4.73–4.88 and 4.92–5.08 (2m, 2H, CH_2N), 5.38–5.54 (m, 1H, CHCl), 6.84–7.06 and 7.18–7.45 (2m, 4H Ar), 8.10 (s, 1H, H-3), 8.68 (s, 1H, H-6). Anal. ($C_{13}H_9N_4Cl_2F$) C, H, N.

7. General Procedure for the Synthesis of 4-Benzylamino Substituted 1-(2-Chloro-2-phenylethyl)- and 1-[2-Chloro-2-(4-halophenyl)ethyl]-1*H*-pyrazolo[3,4-*d*]pyrimidines (9–20). To a solution of **24a**−**c** (10 mmol) in anhydrous toluene (10 mL) was added the appropriate benzylamine (40 mmol), and the mixture was stirred at rt for 48 h. Then, the organic phase was washed with H_2O (2 × 10 mL), dried ($MgSO_4$), and concentrated under reduced

pressure. The crude oil was crystallized by adding a 1:1 mixture of diethyl ether and petroleum ether (bp 40–60 °C).

8. 1-(2-Chloro-2-phenylethyl)-*N*-(4-fluorobenzyl)-1*H*-pyrazolo[3,4-*d*]pyrimidin-4-amine (9). White solid, yield 69%, mp 168–169 °C. ^{1}H NMR: δ 4.62–5.01 (m, 4H, $CH_2N + CH_2Ar$), 5.40–5.54 (m, 1H, CHCl), 6.90–7.44 (m, 9H Ar), 7.80 (s, 1H, H-3), 8.33 (s, 1H, H-6). IR (cm^{-1}): 3247 (NH). Anal. ($C_{20}H_{17}N_5ClF$) C, H, N.

B. Biology. Compound **8** (PP2), used as the reference compound, was purchased from Calbiochem (San Diego, CA).

1. Cell-free Assay with Recombinant Abl. Recombinant human Abl was purchased from Upstate Biotechnology (Waltham, MA) and used to investigate the mechanism of kinase inhibition, as previously reported.[22]

2. Western Blot Analysis. The inhibitory effect of compounds toward the phosphorylation of Bcr-Abl (Tyr245) and STAT-5 (Tyr694) was tested using a PathScan Multiplex Western Detection Kit (Cell Signaling Technology, Beverly, MA). This kit was used to assay the inhibition of multiple proteins on one membrane without stripping and reprobing. The inhibitory effect toward the phosphorylation of Src (Tyr416) was assessed using specific antibodies (Cell Signaling Technology). K-562 and KU-812 were cultured at a concentration of 2.5×10^5 cells/mL and challenged with the compound (50 μM) for 3 h. Later, cells were harvested and lysed in an appropriate buffer containing 1% Triton X-100. Proteins were quantitated by the BCA method (Pierce, Rockford, IL). Equal amounts of total cellular protein were resolved by SDS-polyacrylamide gel electrophoresis, transferred to nitrocellulose filters, and subjected to immunoblot. Nonsaturated, immunoreactive bands were detected with a CCD camera gel documentation system (ChemiDocXRS, Bio-Rad Laboratories, Hercules, CA) and then quantitated with Quantity One analysis software (Bio-Rad Laboratories). The results were expressed as the mean ± SEM of three independent experiments. Statistical analyses were performed using Student's *t* test and the Bonferroni's correction.

3. mRNA Expression of Apoptotic Genes. The mRNA expression of apoptotic genes was performed using qRT-PCR. K-562 and KU-812 cells were cultured at a concentration of 2.5×10^5 cells/mL and challenged with the compound for 3 h and 72 h. Later, the cells were harvested and lysed in an appropriate buffer (RNA wiz, Ambion, Austin, CA). The extract was processed for the extraction of mRNA. For qRT-PCR analysis, *Bcl-xL* (antiapoptotic gene) and *bax* (proapoptotic gene) expression in K-562 and KU-812 cells was determined using a MJ MiniOpticon Cycler (Bio-Rad Laboratories). First-strand cDNA synthesis was performed using iScript cDNA Synthesis Kit (Bio-Rad Laboratories). qRT-PCR was performed using iTaq SYBR Green Supermix with ROX (Bio-Rad Laboratories) and specific primers from GenBank. Data were quantitatively analyzed on an MJ OpticonMonitor detection system (Bio-Rad Laboratories). All values were expressed as fold increase relative to the expression of β-Actin.

C. Computational Details. The protein structure, as well as those of all the ligands, was prepared for computational studies according to procedures previously described.[22] Due to the fact that the biological evaluation of all the chiral compounds reported here was carried out using racemic mixtures, docking analysis was performed on both *R*- and *S*-enantiomers. However, the chirality of the compounds did not affect their binding modes. In particular, the locations of the N1 and C4 side chains within HRI and HRII, respectively, were found unchanged in all the simulations, independently from the stereochemistry of the stereocenter. For graphical purposes, *R*-enantiomers were arbitrarily used to generate pictures showing docking results.

Computation of MIFs within the ATP binding pocket of Abl was carried out with the software Grid (further details in Supporting Information). MIFs were computed for C3, Cl, and F probes. Threshold values of −2 kcal/mol were used for all the three probes.

Acknowledgment. Financial support provided by the Italian MIUR (PRIN 2004_059221 and PRIN 2006_030948) and by the Fondazione Monte dei Paschi di Siena is gratefully acknowledged. Prof. Gabriele Cruciani (University of Perugia, Italy) is also acknowledged for kindly providing us with the programs Grid and VolSurf. We thank Dr. Giovanni Gaviraghi (Sienabiotech S.p.A., Siena, Italy) for helpful discussions.

Supporting Information Available: Details on synthesis, biological assays, molecular modeling, and a table of the elemental analysis data of the new compounds. This material is available free of charge via the Internet at http://pubs.acs.org.

References

(1) Nowell, P. C.; Hungerford, D. A. A minute chromosome in chronic granulocytic leukemia. *Science* **1960**, *132*, 1497–1501.
(2) Rowley, J. D. Letter: a new consistent chromosomal abnormality in chronic myelogenous leukemia identified by quinacrine fluorescence and Giemsa staining. *Nature* **1973**, *243*, 290–293.
(3) Sawyers, C. L. Chronic myeloid leukemia. *N. Engl. J. Med.* **1999**, *340*, 1330–1340.
(4) Lugo, T. G.; Pendergast, A. M.; Muller, A. J.; Witte, O. N. Tyrosine kinase activity and transformation potency of Bcr-Abl oncogene products. *Science* **1990**, *247*, 1079–1082.
(5) Wilson, M. B.; Schreiner, S. J.; Choi, H. J.; Kamens, J.; Smithgall, T. E. Selective pyrrolo-pyrimidine inhibitors reveal a necessary role for Src family kinases in Bcr-Abl signal transduction and oncogenesis. *Oncogene* **2002**, *21*, 8075–8088.
(6) Druker, B. J.; Tamura, S.; Buchdunger, E.; Ohno, S.; Segal, G. M.; Fanning, S.; Zimmermann, J.; Lydon, N. B. Effects of a selective inhibitor of the Abl tyrosine kinase on the growth of Bcr-Abl positive cells. *Nat. Med.* **1996**, *5*, 561–556.
(7) Hochhaus, A.; Kreil, S.; Corbin, A. S.; La Rosee, P.; Muller, M. C.; Lahaye, T.; Hanfstein, B.; Schoch, C.; Cross, N. C.; Berger, U.; Gschaidmeier, H.; Druker, B. J.; Hehlmann, R. Molecular and chromosomal mechanisms of resistance to imatinib (STI571) therapy. *Leukemia* **2002**, *16*, 2190–2196.
(8) Gorre, M. E.; Mohammed, M.; Ellwood, K.; Hsu, N.; Paquette, R.; Rao, P. N.; Sawyers, C. L. Clinical resistance to STI-571 cancer therapy caused by BCR-ABL gene mutation or amlification. *Science* **2001**, *293*, 876–880.
(9) Walz, C.; Sattler, M. Novel targeted therapies to overcome imatinib mesylate resistance in chronic myeloid leukemia (CML). *Crit. Rev. Oncol. Hematol.* **2006**, *57*, 145–164.
(10) Weisberg, E.; Manley, P. W.; Breitenstein, W.; Bruggen, J.; Cowan-Jacob, S. W.; Ray, A.; Huntly, B.; Fabbro, D.; Fendrich, G.; Hall-Meyers, E.; Kung, A. L.; Mestan, J.; Daley, G. Q.; Callahan, L.; Catley, L.; Cavazza, C.; Azam, M.; Neuberg, D.; Wright, R. D.; Gilliland, D. G.; Griffin, J. D. Characterization of AMN107, a selective inhibitor of native and mutant Bcr-Abl. *Cancer Cell* **2005**, *7*, 129–141.
(11) Gumireddy, K.; Baker, S. J.; Cosenza, S. C.; John, P.; Kang, A. D.; Robell, K. A.; Reddy, M. V.; Reddy, E. P. A non-ATP-competitive inhibitor of BCR-ABL overrides imatinib resistance. *Proc. Natl. Acad. Sci. U.S.A.* **2005**, *102*, 1992–1997.
(12) Martinelli, G.; Soverini, S.; Rosti, G.; Baccarani, M. Dual tyrosine kinase inhibitors in chronic myeloid leukemia. *Leukemia* **2005**, *19*, 1872–1879.
(13) Boschelli, D. H. Dual inhibitors of Src and Abl tyrosine kinases. *Drug Des. Rev.—Online* **2004**, *1*, 203–214.
(14) Schenone, S.; Manetti, F.; Botta, M. Synthetic Src-kinase domain inhibitors and their structural requirements. *Anti-Cancer Agents Med. Chem.* **2007**, *7*, 660–680.
(15) (a) Lombardo, L. J.; Lee, F. Y.; Chen, P.; Norris, D.; Barrish, J. C.; Behnia, K.; Castaneda, S.; Cornelius, L. A.; Das, J.; Doweyko, A. M.; Fairchild, C.; Hunt, J. T.; Inigo, I.; Johnston, K.; Kamath, A.; Kan, D.; Klei, H.; Marathe, P.; Pang, S.; Peterson, R.; Pitt, S.; Schieven, G. L.; Schimdt, R. J.; Tokarski, J.; Wen, M. L.; Wityak, J.; Borzilleri, R. M. Discovery of *N*-(2-chloro-6-methyl- phenyl)-2-(6-(4-(2-hydroxyethyl)-piperazin-1-yl)-2-methylpyrimidin-4-ylamino)thiazole-5-carboxamide (BMS-354825), a dual Src/Abl kinase inhibitor with potent antitumor activity in preclinical assays. *J. Med. Chem.* **2004**, *47*, 6658–6661. (b) Das, J.; Chen, P.; Norris, D.; Padmanabha, R.; Lin, J.; Moquin, R. V.; Shen, Z.; Cook, L. S.; Doweyko, A. M.; Pitt, S.; Pang, S.; Shen, D. R.; Fang, Q.; de Fex, H. F.; McIntyre, K. W.; Shuster, D. J.; Gillooly, K. M.; Behnia, K.; Schieven, G. L.; Wityak, J.; Barrish, J. C. 2-Aminothiazole as a novel kinase inhibitor template. Structure-activity relationship studies toward the discovery of *N*-(2-chloro-6-methylphenyl)-2-[[6-[4-(2-hydroxyethyl)-1-piperazinyl)]-2-methyl-4-pyrimidinyl]amino)]-1,3-thiazole-5-carboxamide (dasatinib,

BMS-354825) as a potent pan-Src kinase inhibitor. *J. Med. Chem.* **2006**, *49*, 6819–6832.

(16) (a) Talpaz, M.; Shah, N. P.; Kantarjian, H.; Donato, N.; Nicoll, J.; Paquette, R.; Cortes, J.; O'Brien, S.; Nicaise, C.; Bleickardt, E.; Blackwood-Chirchir, M. A.; Iyer, V.; Chen, T. T.; Huang, F.; Decillis, A. P.; Sawyers, C. L. Dasatinib in imatinib-resistant Philadelphia chromosome-positive leukemias. *N. Engl. J. Med.* **2006**, *354*, 2531–2541. (b) Kolb, E. A.; Gorlick, R.; Houghton, P. J.; Morton, C. L.; Lock, R. B.; Tajbakhsh, M.; Reynolds, C. P.; Maris, J. M.; Keir, S. T.; Billups, C. A.; Smith, M. A. Initial testing of dasatinib by the pediatric preclinical testing program. *Pediatr. Blood Cancer*, http://dx.doi.org/10.1002/pbc.21368.

(17) U.S. Food and Drug Administration. http://www.fda.gov/bbs/topics/NEWS/2006/NEW01400.html (accessed 2006).

(18) Azam, M.; Nardi, V.; Shakespeare, W. C.; Metcalf, C. A., III; Bohacek, R. S.; Wang, Y.; Sundaramoorthi, R.; Sliz, P.; Veach, D. R.; Bornmann, W. G.; Clarkson, B.; Dalgarno, D. C.; Sawyer, T. K.; Daley, G. Q. Activity of dual SRC-ABL inhibitors highlights the role of BCR/ABL kinase dynamics in drug resistance. *Proc. Natl. Acad. Sci. U.S.A.* **2006**, *103*, 9244–9249.

(19) Kimura, S.; Naito, H.; Segawa, H.; Kuroda, J.; Yuasa, T.; Sato, K.; Yokota, A.; Kamitsuji, Y.; Kawata, E.; Ashihara, E.; Nakaya, Y.; Naruoka, H.; Wakayama, T.; Nasu, K.; Asaki, T.; Niwa, T.; Hirabayashi, K.; Maekawa, T. NS-187, a potent and selective dual Bcr-Abl/Lyn tyrosine kinase inhibitor, is a novel agent for imatinib-resistant leukemia. *Blood* **2005**, *106*, 3948–3954.

(20) Naito, H.; Kimura, S.; Nakaya, Y.; Naruoka, H.; Kimura, S.; Ito, S.; Wakayama, T.; Maekawa, T.; Hirabayashi, K. In vivo antiproliferative effect of NS-187, a dual Bcr-Abl/Lyn tyrosine kinase inhibitor, on leukemic cells harbouring Abl kinase domain mutations. *Leuk. Res.* **2006**, *11*, 1443–1446.

(21) Cheetham, G. M.; Charlton, P. A.; Golec, J. M.; Pollard, J. R. Structural basis for potent inhibition of the Aurora kinases and a T315I multidrug resistant mutant form of Abl kinase by VX-680. *Cancer Lett.* **2007**, *251*, 323–329.

(22) Manetti, F.; Pucci, A.; Magnani, M.; Locatelli, G. A.; Brullo, C.; Naldini, A.; Schenone, S.; Maga, G.; Carraro, F.; Botta, M. Inhibition of Bcr-Abl phosphorylation and induction of apoptosis by pyrazolo[3,4-*d*]pyrimidines in human leukemia cells. *ChemMedChem* **2007**, *2*, 343–353.

(23) *Grid 22*; Molecular Discovery Ltd: Pinner, Middlesex, U.K.

(24) (a) Cruciani, G.; Pastor, M.; Guba, W. Volsurf: a new tool for the pharmacokinetic optimization of lead compounds. *Eur. J. Pharm. Sci.* **2000**, *11* (2), S29–S39. (b) Further information at the Volsurf web site: http://www.moldiscovery.com/docs/volsurf.

(25) Carraro, F.; Naldini, A.; Pucci, A.; Locatelli, G. A.; Maga, G.; Schenone, S.; Bruno, O.; Ranise, A.; Bondavalli, F.; Brullo, C.; Fossa, P.; Menozzi, G.; Mosti, L.; Modugno, M.; Tintori, C.; Manetti, F.; Botta, M. Pyrazolo[3,4-*d*]pyrimidines as potent antiproliferative and proapoptotic agents toward A431 and 8701-BC cells in culture via inhibition of c-Src phosphorylation. *J. Med. Chem.* **2006**, *49*, 1549–1561.

(26) Schenone, S.; Brullo, C.; Bruno, O.; Bondavalli, F.; Ranise, A.; Botta, M.; Corradi, V.; Santucci, M. A.; Mancini, M.; Corrado, P.; Crespan, E.; Maga, G. Synthesis of new pyrazolo[3,4-*d*]pyrimidines Bcr-Abl tyrosine kinase inhibitors. XVIII Convegno Nazionale della Divisione di Chimica Farmaceutica della Società Chimica Italiana: Chieti-Pescara, Italy, September 16–20, 2007; Abs. P-113.

JM701240C